

Proceeding Paper

# Synthesis of $\text{Ti}_3\text{C}_2\text{T}_x/\text{TiO}_2$ Nanowires for Ascorbic Acid, Dopamine, and Uric Acid Simultaneous Sensing <sup>†</sup>

Tao Yang <sup>1,2,\*</sup> , Dengzhou Jia <sup>1,2</sup> and Xinmei Hou <sup>1,2</sup>

<sup>1</sup> Institute for Carbon Neutrality, University of Science and Technology Beijing, Beijing 100083, China; dengzhoujia@163.com (D.J.); houxinmei@163.com (X.H.)

<sup>2</sup> Institute of Steel Sustainable Technology, Liaoning Academy of Materials, Shenyang 110000, China

\* Correspondence: yangtaoustb@ustb.edu.cn

<sup>†</sup> Presented at the 2nd International Electronic Conference on Chemical Sensors and Analytical Chemistry, 16–30 September 2023; Available online: <https://csac2023.sciforum.net/>.

**Abstract:** The development of electrochemical sensors with high sensitivity for the simultaneous detection of ascorbic acid (AA), dopamine (DA), and uric acid (UA) is urgently desirable in clinical medicine. However, the challenge lies in achieving simultaneous detection due to their close oxidation potentials. In this work, we present the synthesis of a composite material comprised of in situ-grown  $\text{TiO}_2$  nanowires (NWs) on a  $\text{Ti}_3\text{C}_2\text{T}_x$  substrate ( $\text{Ti}_3\text{C}_2\text{T}_x/\text{TiO}_2$  NWs) through a facile alkali process. By modifying a glassy carbon electrode (GCE) with  $\text{Ti}_3\text{C}_2\text{T}_x/\text{TiO}_2$  NWs ( $\text{Ti}_3\text{C}_2\text{T}_x/\text{TiO}_2$  NWs/GCE), it showed excellent electrocatalytic activity for the simultaneous detection of AA/DA/UA by regulating the surface functional groups of  $\text{Ti}_3\text{C}_2\text{T}_x$ . Remarkably, the  $\text{Ti}_3\text{C}_2\text{T}_x/\text{TiO}_2$  NWs/GCE enabled simultaneous detection of AA in the range of 300–1800  $\mu\text{M}$ , DA in the range of 2–33  $\mu\text{M}$ , and UA in the range of 2–33  $\mu\text{M}$ . The limits of detection (LODs) for AA, DA, and UA were estimated as 66.07  $\mu\text{M}$ , 0.023  $\mu\text{M}$ , and 0.011  $\mu\text{M}$ , respectively. The proposed  $\text{Ti}_3\text{C}_2\text{T}_x/\text{TiO}_2$  NWs/GCE demonstrated good stability, high selectivity, and reliable reproducibility, making it a promising electrochemical sensor for the detection of AA, DA, and UA. This work offers a new perspective for human health monitoring, paving the way for advancements in this field.

**Keywords:**  $\text{Ti}_3\text{C}_2\text{T}_x$ ;  $\text{TiO}_2$ ; ascorbic acid; dopamine; uric acid; electrochemical sensor



**Citation:** Yang, T.; Jia, D.; Hou, X.

Synthesis of  $\text{Ti}_3\text{C}_2\text{T}_x/\text{TiO}_2$  Nanowires for Ascorbic Acid, Dopamine, and Uric Acid Simultaneous Sensing. *Eng. Proc.* **2023**, *48*, 19. <https://doi.org/10.3390/CSAC2023-14905>

Academic Editor: Nicole Jaffrezic-Renault

Published: 26 September 2023



**Copyright:** © 2023 by the authors. Licensee MDPI, Basel, Switzerland. This article is an open access article distributed under the terms and conditions of the Creative Commons Attribution (CC BY) license (<https://creativecommons.org/licenses/by/4.0/>).

## 1. Introduction

Ascorbic acid (AA), dopamine (DA), and uric acid (UA) coexist in body fluids, with basal concentrations ranging from 100 to 1400  $\mu\text{M}$ , 0.01 to 1  $\mu\text{M}$ , and 200 to 500  $\mu\text{M}$ , respectively. They are three essential biomolecules coexisting in body fluids that play vital roles in regulating various physiological functions [1]. Fluctuations in the levels of these biomolecules have been linked to various common ailments such as skin rashes, Alzheimer's disease, Parkinson's disease, and gout [2,3]. Therefore, the rapid and accurate simultaneous detection of AA, DA, and UA concentrations in body fluids plays a crucial role in disease diagnoses [4,5]. In this work, a composite of  $\text{TiO}_2$  nanowires grown in situ on  $\text{Ti}_3\text{C}_2\text{T}_x$  ( $\text{Ti}_3\text{C}_2\text{T}_x/\text{TiO}_2$  NWs) was synthesized through a simple alkali treatment. By regulating the surface functional groups and incorporating  $\text{TiO}_2$ , the  $\text{Ti}_3\text{C}_2\text{T}_x/\text{TiO}_2$ -NW-modified electrode achieved the individual and simultaneous detections of AA, DA, and UA. Furthermore, the proposed  $\text{Ti}_3\text{C}_2\text{T}_x/\text{TiO}_2$  NWs/GCE exhibited excellent stability, selectivity, reproducibility, and repeatability.

## 2. Result and Discussion

### 2.1. Characterization of $\text{Ti}_3\text{C}_2\text{T}_x/\text{TiO}_2$ NWs

SEM images in Figure 1e–g depict the  $\text{Ti}_3\text{C}_2\text{T}_x$  treated in a 6 M KOH solution for 10, 20, and 30 h, respectively. After 10 h of alkaline treatment, only a few NWs can be

observed growing between the  $\text{Ti}_3\text{C}_2\text{T}_x$  lamellae (Figure 1a). Subsequently, after 20 h of alkali treatment, the number of NWs significantly increases (Figure 1b). Moreover, as shown in Figure 1c, the NWs start to clump together after 30 h of alkali treatment. TEM and high-resolution TEM images in Figure 1d–f display the  $\text{Ti}_3\text{C}_2\text{T}_x$  treated in a 6 M KOH solution for 20 h. NWs with lengths ranging from 350 to 450 nm and diameters of 10–35 nm grow on the surfaces and edges of the  $\text{Ti}_3\text{C}_2\text{T}_x$  lamellae (Figure 1d). The lattice fringe spacing of the lamellae is determined to be 0.253 nm, which corresponds to the (002) crystal plane of  $\text{Ti}_3\text{C}_2\text{T}_x$  (Figure 1e). Additionally, the lattice fringe spacing of the NWs is measured to be 0.352 nm, in alignment with the (101) crystal plane of anatase  $\text{TiO}_2$  (Figure 1f) [6].

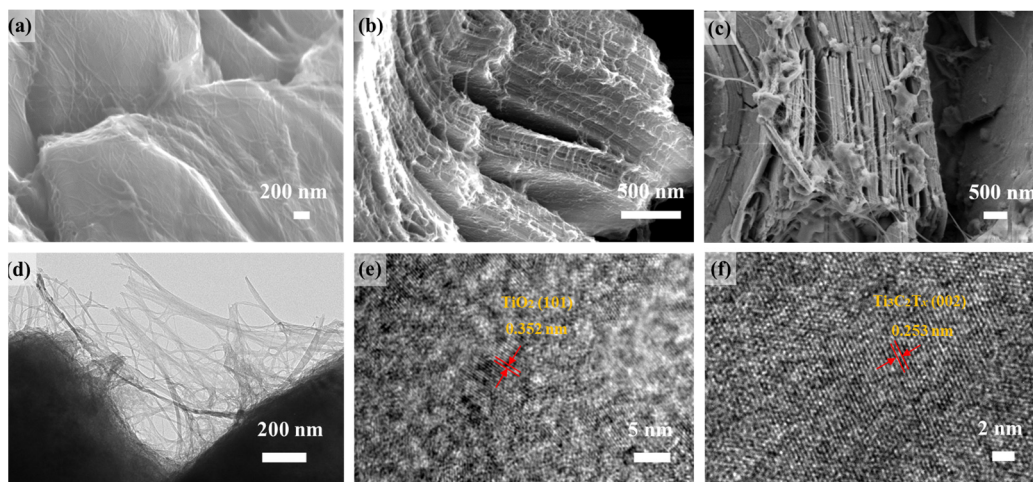


**Figure 1.**  $\text{Ti}_3\text{C}_2\text{T}_x$  treated at 6 M KOH for (a) 10 h, (b) 20 h, and (c) 30 h; 20h- $\text{Ti}_3\text{C}_2\text{T}_x/\text{TiO}_2$  NW (d) TEM image and (e,f) HR-TEM image.

## 2.2. Simultaneous Measurement of AA, DA, and UA with DPV

Figure 2 demonstrates the simultaneous detection of AA, DA, and UA with DPV on the  $\text{Ti}_3\text{C}_2\text{T}_x/\text{TiO}_2$  NWs/GCE, with a scan rate of  $50 \text{ mV s}^{-1}$ . Figure 2a exhibits distinct oxidation peak potentials for AA, DA, and UA, measuring 0.18 V, 0.32 V, and 0.59 V, respectively. A linear relationship between the peak currents and concentrations is observed in the range of 300–1800  $\mu\text{M}$  for AA, yielding an  $R^2$  value of 0.9953 (Figure 2b). Similarly, for DA, multiple linear segments are observed within the concentration ranges of 2–9  $\mu\text{M}$  and 9–33  $\mu\text{M}$ , resulting in  $R^2$  values of 0.9930 and 0.9943, respectively (Figure 2c). For UA, multiple linear segments are observed within the concentration ranges of 2–7  $\mu\text{M}$  and 7–33  $\mu\text{M}$ , yielding  $R^2$  values of 0.9860 and 0.9977, respectively (Figure 2d). The LODs for AA, DA, and UA are estimated to be 66.07  $\mu\text{M}$ , 0.023  $\mu\text{M}$ , and 0.011  $\mu\text{M}$ , respectively.

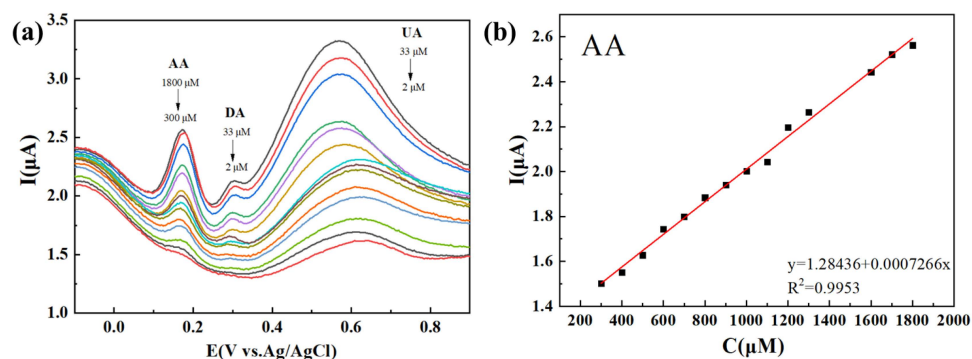


**Figure 2.** Cont.

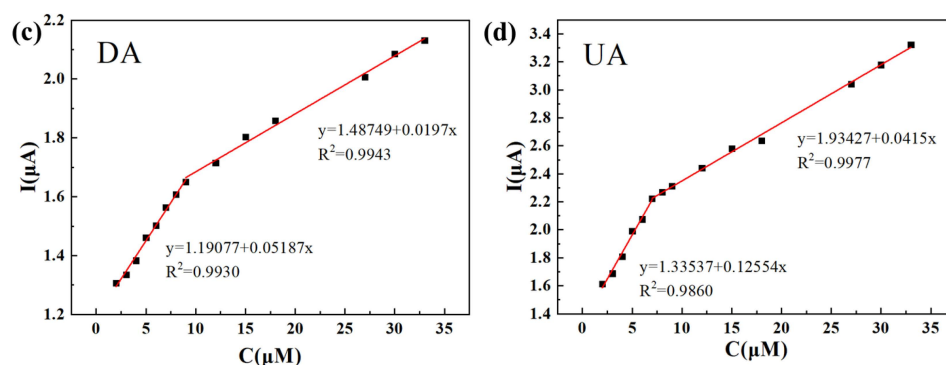


**Figure 2.** (a) DPVs recorded for different concentrations of AA, DA, and UA at the  $\text{Ti}_3\text{C}_2\text{T}_x/\text{TiO}_2$  NWs/GCE in 0.1 M PBS (pH 7.4) upon successive additions from 300 to 1800  $\mu\text{M}$  for AA, 2 to 33  $\mu\text{M}$  for DA, and 2 to 33  $\mu\text{M}$  for UA. (b–d) The calibration curves made for DA, UA and AA from their oxidation peak currents vs. concentrations.

### 3. Conclusions

In summary, the  $\text{Ti}_3\text{C}_2\text{T}_x/\text{TiO}_2$ -NW-modified GCE demonstrated the simultaneous detection of AA (300–1800  $\mu\text{M}$ ), DA (2–33  $\mu\text{M}$ ), and UA (2–33  $\mu\text{M}$ ) with LODs of 66.07  $\mu\text{M}$  (AA), 0.023  $\mu\text{M}$  (DA), and 0.011  $\mu\text{M}$  (UA). The surface of  $\text{Ti}_3\text{C}_2\text{T}_x$  exhibited neutral properties due to the substitution of hydroxyl groups with fluorine groups after alkali treatment. Moreover, the active surface area of the  $\text{Ti}_3\text{C}_2\text{T}_x/\text{TiO}_2$  NWs/GCE (0.39  $\text{cm}^2$ ) was approximately five times larger than that of the bare GCE (0.08  $\text{cm}^2$ ) due to the in situ generation of  $\text{TiO}_2$  NWs on  $\text{Ti}_3\text{C}_2\text{T}_x$ . The distinct separation of the detection peaks for AA, DA, and UA can be attributed to the enhanced transition of charge carriers at the heterojunctions of  $\text{Ti}_3\text{C}_2\text{T}_x$  and  $\text{TiO}_2$ . Overall, the electrochemical sensor based on  $\text{Ti}_3\text{C}_2\text{T}_x/\text{TiO}_2$  NWs exhibits exceptional anti-interference ability, stability, and reliable reproducibility.

**Author Contributions:** Conceptualization, T.Y. and D.J.; methodology, T.Y. and X.H.; validation, D.J. and X.H.; formal analysis, D.J. and T.Y.; investigation, X.H.; data curation, D.J.; writing—original draft preparation, D.J. and T.Y.; writing—review and editing, X.H.; supervision, X.H.; project administration, X.H.; funding acquisition, T.Y. and X.H. All authors have read and agreed to the published version of the manuscript.

**Funding:** This work was supported by the National Science Fund for Distinguished Young Scholars (No. 52025041), the National Natural Science Foundation of China (No. 51902020, 51974021, 52250091), the Fundamental Research Funds for the Central Universities of NO. FRF-TP-20-02C2. This project is supported by State Key Laboratory of Featured Metal Materials and Life-cycle Safety for Composite Structures, Guangxi University (Grant No. 2021GXYSOF12), and the Interdisciplinary Research Project for Young Teachers of USTB (Fundamental Research Funds for the Central Universities) (NO. FRF-IDRY-21-028).

**Institutional Review Board Statement:** Not applicable.

**Informed Consent Statement:** Not applicable.

**Data Availability Statement:** Data available on request due to privacy or ethical restrictions. The data presented in this study are available on request from the corresponding author.

**Conflicts of Interest:** The authors declare no conflict of interest.

### References

- Zhang, W.; Liu, L.; Li, Y.; Wang, D.; Ma, H.; Ren, H.; Shi, Y.; Han, Y.; Ye, B.-C. Electrochemical sensing platform based on the biomass-derived microporous carbons for simultaneous determination of ascorbic acid, dopamine, and uric acid. *Biosens. Bioelectron.* **2018**, *121*, 96–103. [[CrossRef](#)] [[PubMed](#)]
- Shang, N.G.; Papakonstantinou, P.; McMullan, M.; Chu, M.; Stamboulis, A.; Potenza, A.; Dhessi, S.S.; Marchetto, H. Catalyst-Free Efficient Growth, Orientation and Biosensing Properties of Multilayer Graphene Nanoflake Films with Sharp Edge Planes. *Adv. Funct. Mater.* **2008**, *18*, 3506–3514. [[CrossRef](#)]

3. Habibi, B.; Pournaghi-Azar, M.H. Simultaneous determination of ascorbic acid, dopamine and uric acid by use of a MWCNT modified carbon-ceramic electrode and differential pulse voltammetry. *Electrochim. Acta* **2010**, *55*, 5492–5498. [[CrossRef](#)]
4. Yan, J.; Liu, S.; Zhang, Z.; He, G.; Zhou, P.; Liang, H.; Tian, L.; Zhou, X.; Jiang, H. Simultaneous electrochemical detection of ascorbic acid, dopamine and uric acid based on graphene anchored with Pd-Pt nanoparticles. *Colloids Surf. B* **2013**, *111*, 392–397. [[CrossRef](#)]
5. Lee, H.C.; Chen, T.H.; Tseng, W.L.; Lin, C.H. Novel core etching technique of gold nanoparticles for colorimetric dopamine detection. *Analyst* **2012**, *137*, 5352–5357. [[CrossRef](#)]
6. Cao, M.; Wang, F.; Wang, L.; Wu, W.; Lv, W.; Zhu, J. Room Temperature Oxidation of  $Ti_3C_2$ MXene for Supercapacitor Electrodes. *J. Electrochem. Soc.* **2017**, *164*, A3933–A3942. [[CrossRef](#)]

**Disclaimer/Publisher's Note:** The statements, opinions and data contained in all publications are solely those of the individual author(s) and contributor(s) and not of MDPI and/or the editor(s). MDPI and/or the editor(s) disclaim responsibility for any injury to people or property resulting from any ideas, methods, instructions or products referred to in the content.